The Molecular Basis of the Solution Properties of Hyaluronan Investigated by Confocal Fluorescence Recovery After Photobleaching

Philip Gribbon, Boon C. Heng, and Timothy E. Hardingham
Wellcome Trust Centre for Cell-Matrix Research, School of Biological Sciences, University of Manchester, Manchester M13 9PT, United Kingdom

ABSTRACT Hyaluronan (HA) is a highly hydrated polyanion, which is a network-forming and space-filling component in the extracellular matrix of animal tissues. Confocal fluorescence recovery after photobleaching (confocal-FRAP) was used to investigate intramolecular hydrogen bonding and electrostatic interactions in hyaluronan solutions. Self and tracer lateral diffusion coefficients within hyaluronan solutions were measured over a wide range of concentrations (*c*), with varying electrolyte and at neutral and alkaline pH. The free diffusion coefficient of fluoresceinamine-labeled HA of 500 kDa in PBS was 7.9×10^{-8} cm^2 s^{-1} and of 830 kDa HA was 5.6×10^{-8} cm^2 s^{-1}. Reductions in self- and tracer-diffusion with *c* followed a stretched exponential model. Electrolyte-induced polyanion coil contraction and destiffening resulted in a 2.8-fold increase in self-diffusion between 0 and 100 mM NaCl. Disruption of hydrogen bonds by strong alkali (0.5 M NaOH) resulted in further larger increases in self- and tracer-diffusion coefficients, consistent with a more dynamic and permeable network. Concentrated hyaluronan solution properties were attributed to hydrodynamic and entanglement interactions between domains. There was no evidence of chain-chain associations. At physiological electrolyte concentration and pH, the greatest contribution to the intrinsic stiffness of hyaluronan appeared to be due to hydrogen bonds between adjacent saccharides.

INTRODUCTION

Hyaluronan (HA) is a high molecular weight (up to 5×10^6) linear glycosaminoglycan (GAG), composed of N-acetyl-D-glucosamine (GlcNAc) and D-glucuronic acid (GlcA) that form the disaccharide repeat (-GlcNAc-β1, 4-GlcA-β1, 3) (Laurent, 1995; Scott, 1992). HA is a major component of the extracellular matrix (ECM) of vertebrate tissues and is a space-filling molecule that also acts as a scaffold for the binding of other matrix macromolecules (Fosang and Hardingham, 1996). The hydrodynamic and network properties of HA have a profound influence on the transport and biomechanical properties of many biological tissues (Coleman et al., 1998; Comper and Zamparo, 1990).

Previously, the properties of HA, particularly in dilute solution, have been investigated by a range of techniques (Cleland, 1968; Sheehan et al., 1983; Reed and Reed, 1989). However, because of experimental limitations, especially with techniques such as dynamic light scattering (DLS), anomalies in the reported properties persist, which hinder a more complete interpretation of the behavior of HA.

Measurements of lateral self- and tracer-diffusion coefficients by confocal fluorescence recovery after photobleaching (confocal-FRAP) provide a powerful method for determining concentrated solution properties in the absence of flow and shear forces (Kubitscheck et al., 1994; Gribbon and Hardingham, 1998). Confocal-FRAP is also applicable to the study of concentrated, complex mixtures of macromolecules such as found in the ECM. In previous work the concentrated solution properties of aggrecan and the more stable networks formed when aggrecan is aggregated with HA were investigated by confocal-FRAP (Gribbon and Hardingham, 1998). The pore dimensions of HA matrices have been determined by conventional FRAP tracer-diffusion measurements using dextran probes (De Smedt et al., 1994). In this study, in order to understand how electrostatic interactions and hydrogen bonding of HA contribute to its properties in solution, the self-diffusion coefficient of HA was determined over a range of macromolecular concentrations, counterion concentrations, and at neutral and alkaline pH (Morris et al., 1980; Ghosh et al., 1990). The characteristics of HA networks formed under different conditions were also investigated by measuring the permeability to an uncharged dextran macromolecular probe.

MATERIALS AND METHODS

Fluorescent labeling of HA

HA extracted from cock's comb was supplied by Seikagaku Corp. (Tokyo, Japan, batches HMT0039 and TH1003). Samples in deionized water were made up in PBS (0.01 M sodium phosphate, 0.0027 M KCl, 0.137 M NaCl, pH 7.4). Molecular weights were determined by size exclusion column chromatography (Sephacryl S-1000, Pharmacia, Uppsala, Sweden, 16 × 1000 mm, 0.5 ml/min) coupled with on-line multiangle laser light scattering (MALLS) and a differential refractometer (Dawn DSP, Wyatt Technology, Santa Barbara, CA) (Reed, 1996). The refractive increment (d*n*/d*c*) used in the analysis was 0.15 ml/g (Sheehan et al., 1983) and the second virial coefficient was 2.5×10^{-3} mL/mol/g^2 (Ghosh et al., 1993). Batches HMT0039 and TH1003 gave weight-average molecular weights (M_w) of $0.93 \pm 0.06 \times 10^6$ and $2.05 \pm 0.05 \times 10^6$ (mean ± SE, $n = 2$), respectively. Corresponding weight-averaged radii of gyration (R_g) were 100.6 ± 4.7 nm and 157.4 ± 4.4 nm (mean ± SE, $n = 2$). For both samples, the ratio of weight-averaged molecular weight to number-averaged molecular weight (polydispersity index) was 1.3. Protein present was <0.1% (w/w) of HA (BCA protein assay, Pierce, IL).

Received for publication 11 March 1999 and in final form 9 July 1999.

Address reprint requests to Dr. Timothy E. Hardingham, Wellcome Trust Centre for Cell Matrix Research, School of Biological Sciences, University of Manchester, Manchester M13 9PT, UK. Tel.: 44-161-275-5511; Fax: 44-161-275-5082; E-mail: timothy.e.hardingham@man.ac.uk.

© 1999 by the Biophysical Society

0006-3495/99/10/2210/07 $2.00

HA (930 kDa) was labeled with fluoresceinamine (FA) (Glabe et al., 1983). HA (1 mg/ml) was activated by the addition of an equal volume of CNBr (1 mg/ml), at 4°C. The pH was maintained at 11 by the addition of NaOH (1 M) and after 5 min and 30 min, activated HA was separated from unreacted CNBr by size exclusion (Hi-Trap, Pharmacia, Uppsala, Sweden, 0.2 M borate buffer, pH 8.0). The activated HA was reacted at 4°C for 24 h with a 20-fold molar excess of FA. Unbound FA and buffer salts were removed by membrane separation (Centriplus-100, Amicon) and the FA-HA (sodium salt) was freeze-dried to constant mass. Size exclusion chromatography (S-1000) of the FA-HA showed that the label was evenly distributed in all sizes. The labeling efficiency increased with activation time, but it also resulted in some depolymerization. The products prepared with 5- and 30-min activation were 830 ± 30 kDa ($n = 6$), and 500 kDa ($n = 2$), respectively, and corresponding R_g values were 90 and 53 nm. The polydispersity of both samples was 1.4. The absorbance at 490 nm corresponded to between 2 and 3 mol FA per mol of HA. Chromatography of the final products showed no unbound FA.

Preparation of solutions for confocal-FRAP

For studies of the concentration dependence of FA-HA self-diffusion, FA-HA was at 0.05–8 mg/ml in PBS. For ionic strength studies, FA-HA was at 0.2, 2.0, and 10 mg/ml in 1–1000 mM NaCl unbuffered at pH ~ 5.5. The limiting fluorescence of the 830 kDa FA-HA meant experiments at low concentrations (<0.5 mg/ml) used only the 500 kDa preparation. Solutions were equilibrated for at least 48 h at 4°C with gentle rotation. All solutions were prepared by weight and concentrations were confirmed refractometrically. For experiments with NaOH, FA-HA (830 kDa) was equilibrated in deionized water and before confocal-FRAP analysis NaOH was added and solutions mixed for 3 h. In all solutions, ionic strength was maintained at 0.5 M by the addition of NaCl. Incubation in 0.5 M NaOH at 25°C was shown to reduce the weight-averaged molecular weight of HA and FA-HA by <5% in 10 h, and there was no release of FA. To determine the reversibility of alkali effects on self-diffusion properties, FA-HA (830 kDa, 4 mg/ml) was incubated at 25°C in 0.5 M NaOH for 3 h. The sample was placed in an ice bath and neutralized by the addition of an equal volume of 0.5 M HCl containing 20 mM phosphate buffer. For the corresponding control, FA-HA (830 kDa, 4 mg/ml) was incubated in 0.5 M NaCl for 3 h and an equal volume of 20 mM phosphate buffer was added. Both neutralized and control samples were then at 2 mg/ml in 0.25 M NaCl and 10 mM phosphate, pH 7.4. After incubation at 25°C for 1 h their self-diffusion coefficients were determined. In tracer studies, fluoresceine isothiocyanate (FITC)-labeled dextran (M_w = 2000 kDa, polydispersity 1.25, molar ratio FITC/glucose ~0.008), (Sigma, Poole, UK) was added to unlabeled HA with a final tracer concentration of 0.1 mg/ml (Gribbon and Hardingham, 1998).

Diffusion measurements and data analysis

The confocal-FRAP instrumentation and variance recovery analysis were as described previously (Gribbon and Hardingham, 1998; Kubitscheck et al., 1994). Briefly, samples (30 μl) sealed in cavity slides were maintained at 25°C (PE-60, Linkam Instruments, Tadworth, UK). In one set of experiments, diffusion measurements were made over the temperature range 5–60°C. Sample bleaching and recovery fluorescence excitation used the 488-nm line of an argon-ion laser (100 mW) in a BioRad MRC-1000 confocal microscope, (Biorad, Hemel Hempstead, UK) and emitted light was monitored at 520 nm. Prebleach and recovery image scans were at 0.3% of maximum laser power. A square central region (typically 75 × 75 μm) was bleached at maximum laser power. For recovery, a time series of up to 50 recovery images was collected, typically over 1–10 min. For each experiment, the mobile fraction was calculated and in the experiments reported here, no immobile fraction was detected. Lateral self-and tracer-diffusion coefficients (D) were calculated from the time dependence of plots of the second moment of the radially averaged distribution of bleached fluorophores (Kubitscheck et al., 1994). For each condition six replicate experiments were performed and results are presented as mean ± standard deviation.

The extent of photobleaching did not change with pH or ionic strength over the range used, although the sample fluorescence was reduced at low ionic strength and pH. For all samples, analysis of the recovery series showed the expected linear dependence of the second moment of the radial distribution of bleached fluorophore on time. Recovery kinetics were consistent with first-order behavior of a single component.

RESULTS

Self-diffusion of HA

The lateral self-diffusion coefficients were determined for FA-HA of 500 kDa and 830 kDa in PBS, at concentrations extending from below to well above the predicted critical concentration for domain overlap (c^*) (Fig. 1). By using R_g values determined from the MALLS calibrations, c^* values for the 500 and 830 kDa FA-HA were calculated from the relationship $c^* = 3M/(4\pi N_A R_g^3)$ and gave $c^* = 0.43$ mg/ml and 1.31 mg/ml for 500 kDa and 830 kDa, respectively. With both molecular weights, the lateral self-diffusion coefficients reduced steeply with concentration in a manner consistent with phenomenological descriptions of polymer self-diffusion in terms of a universal scaling equation (Phillies, 1989).

$$D = D_0 \exp(-\alpha c^{\nu}) \quad (1)$$

Where D_0 is the polymer free self-diffusion defined in the limit of zero concentration, and α and ν are empirically derived. The parameter α describes the strength of interpolymer hydrodynamic interactions and the deviation of ν from unity arises from chain contraction at high concentrations. Data were fitted to Eq. 1 using a nonlinear least-squares fit (non-weighted). Analysis of data from results with the 830 kDa FA-HA gave $D_0 = 5.6 \times 10^{-8}$ cm^2 s^{-1}, $\alpha = 0.63$ ml/mg, and $\nu = 0.74$. The lower molecular mass HA (500 kDa) gave a higher $D_0 = 7.9 \times 10^{-8}$ cm^2 s^{-1}, $\alpha =$

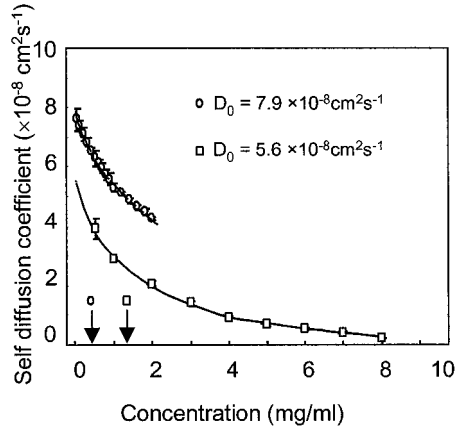

FIGURE 1 Concentration dependence of the lateral translational self-diffusion coefficients of FA-HA, 500 kDa (○), and 830 kDa (□). Vertical arrows show the locations of the c^* (see text). Solid lines show fits to Eq. 1, and are extrapolated to zero concentration. All measurements in PBS at 25°C.

0.38 ml/mg and $\nu = 0.73$. These measurements were insensitive to pH over a broad range (4–8) and also to temperature between 5 and 60°C, when changes in solvent viscosity had been accounted for (data not shown, analysis by two-tailed unpaired Student's *t*-test).

Investigation of the effect of increasing electrolyte concentration on HA solution properties showed that the self-diffusion coefficients of 500 and 830 kDa FA-HA were very low in the presence of low electrolyte, but increased dramatically with small increases in NaCl concentration (Fig. 2). This is consistent with increased electrostatic shielding resulting in polyanion coil contraction, and this effect was largely complete at 100 mM NaCl. Both molecular weight fractions showed a 2.8-fold increase in lateral self-diffusion coefficient from zero to 100 mM added salt.

The effects of alkaline pH were investigated as a method to disrupt hydrogen bond-based chain stiffening (Morris et al., 1980). The FA-HA (500 kDa) was initially analyzed at low concentration (0.2 mg/ml), where the self-diffusion coefficient is 90% of the free solution value (Fig. 1) and transport coefficients are dominated by the properties of single chains. Under these conditions the self-diffusion coefficient was greatly increased in NaOH compared to control experiments in NaCl (Fig. 3). Ionic strength of solutions in NaOH was maintained at 500 mM by the addition of NaCl. Comparable measurements at higher concentrations (2 mg/ml and 10 mg/ml) with FA-HA (830 kDa) in the presence of supporting electrolyte showed correspondingly large increases in self-diffusion with added NaOH (Fig. 4). In 500 mM NaOH the self-diffusion coefficient of FA-HA (830 kDa) was much greater than in 500 mM NaCl, and very much greater than in deionized water, at all HA concentrations (Fig. 5). Data from Fig. 5 were fitted to Eq. 1, and in 500 mM NaOH, $D_0 = 10.3 \times 10^{-8}$ cm^2 s^{-1}, $\alpha = 0.07$ ml/mg, and $\nu = 0.98$; in 500 mM NaCl, $D_0 = 4.9 \times 10^{-8}$ cm^2 s^{-1}, $\alpha = 0.16$ ml/mg, and $\nu = 1.07$; in deionized water, $D_0 = 1.4 \times 10^{-8}$ cm^2 s^{-1}, $\alpha = 0.18$ ml/mg, and $\nu = 0.88$. These data suggest that in strong alkaline conditions at low concentrations, HA has a much smaller domain, and at high concentrations (10 mg/ml) there is much less interchain hydrodynamic interaction than at neutral pH. The effects of alkali incubation were fully reversible upon neutralization. The self-diffusion coefficient for the alkali incubated and neutralized FA-HA was $2.3 \pm 0.2 \times 10^{-8}$ cm^2 s^{-1}, which was not significantly different from the control value of $2.2 \pm 0.1 \times 10^{-8}$ cm^2 s^{-1} ($n = 5$, Student's paired *t*-test).

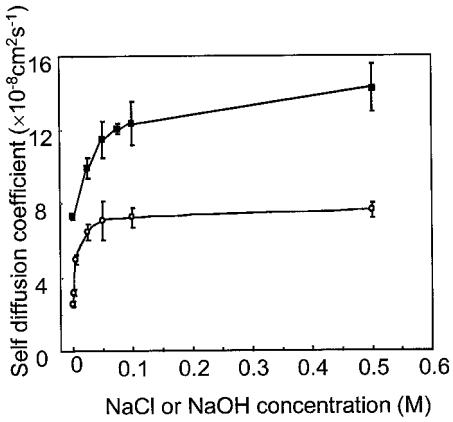

FIGURE 3 Lateral translational self-diffusion coefficient of 500 kDa FA-HA (0.2 mg/ml) versus concentration of added NaCl (○) or NaOH (■). Ionic strength of solutions in NaOH is maintained at 500 mM by the addition of NaCl. All measurements at 25°C.

Tracer diffusion experiments

The effects of supporting electrolyte and high pH conditions on the permeability of HA solutions were investigated using a high molecular mass FITC-dextran probe (2000 kDa). In control experiments the diffusion coefficient of FITC-dextran (2000 kDa) in PBS at zero HA concentration (D_t^0) was $13.1 \pm 0.5 \times 10^{-8}$ cm^2 s^{-1}, $R_h = 19 \pm 1$ nm, and it was

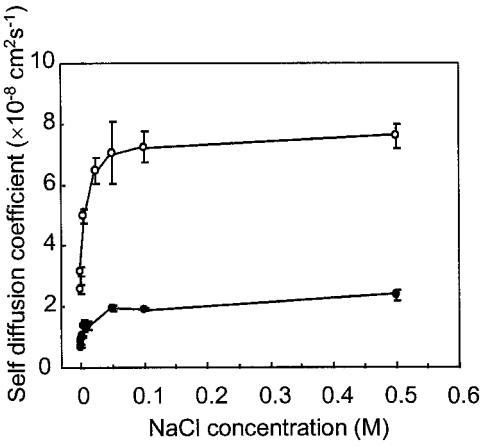

FIGURE 2 Lateral translational self-diffusion coefficient of FA-HA versus concentration of added NaCl for 500 kDa FA-HA at 0.2 mg/ml (○) and 830 kDa HA at 2 mg/ml (●). All measurements at 25°C.

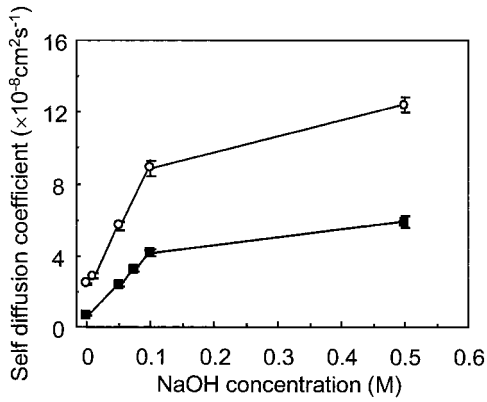

FIGURE 4 Lateral translational self-diffusion coefficient of 830 kDa FA-HA at 2 mg/ml (○) and 10 mg/ml (■) versus concentration of added NaOH. Ionic strength of solutions in NaOH is maintained at 500 mM by the addition of NaCl. All measurements at 25°C.

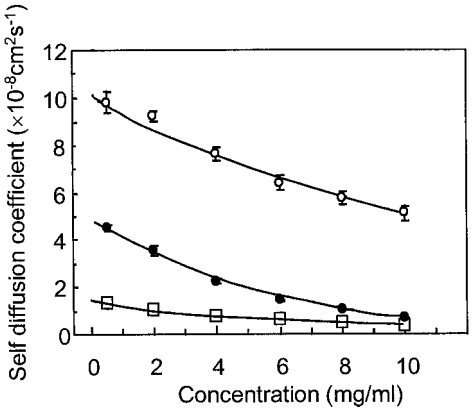

FIGURE 5 Lateral translational self-diffusion coefficient of 830 kDa FA-HA versus concentration of HA for solutions in 500mM NaOH (○), 500 mM NaCl (●), and deionized water (□). All measurements at 25°C.

shown to be independent of NaOH and NaCl concentration (two-tailed unpaired Student's *t*-test).

At low concentration of HA (below 6 mg/ml), the FITC-dextran was more mobile in 930 kDa than in 2050 kDa HA, but at higher concentrations the tracer diffusion coefficient was independent of HA molecular weight (Fig. 6). These data were fitted to the scaling equation for tracer diffusion, which has a similar form to Eq. 1 (Phillies, 1989):

$$D_t = D_t^0 \exp(-\beta c^{\upsilon}) \tag{2}$$

where D_t is the apparent lateral translational tracer diffusion coefficient, and β and υ are empirical constants. In the least-squares, nonlinear fit, β and υ were set as adjustable parameters. For 930 kDa HA, $\beta = 0.19$ ml/mg and $\upsilon = 0.88$; for 2050 kDa HA, $\beta = 0.30$ ml/mg and $\upsilon = 0.66$. The parameters β and υ can be related to the correlation length ξ (De Smedt et al., 1994), which describes the separation between chain entanglement points within a polymeric network (De Gennes, 1974). In real polymer solutions interchain associations are transient and the network is dynamic; therefore, ξ is an averaged dimension representing a distribution of apparent mesh sizes. The expression for ξ is:

$$\xi = \left(\frac{d}{\beta}\right) c^{-\upsilon} \tag{3}$$

where d is the hydrodynamic diameter of the tracer. Plots of correlation length against HA concentration are shown in the inset of Fig. 6, and data from De Smedt et al. are also shown for comparison. At lower concentrations of HA, results with the FITC-dextran (2000 kDa) gave longer correlation lengths than with a lower molecular mass FITC-dextran (487 kDa), indicating some partial size selectivity by the network, but this was not detected at higher HA concentration (>6 mg/ml).

Comparison of the lateral tracer diffusion coefficients of FITC-dextran (2000 kDa) in HA solutions showed that it was highest in 500 mM NaOH, lower in 500 mM NaCl, and lowest in deionized water. Data were fitted to Eq. 2 (Fig. 7, *solid lines*). In water, $D_t^0 = 13.2\ (\pm 0.6) \times 10^{-8}$ cm^2 s^{-1}, $\beta = 0.58$ ml/mg, and $\upsilon = 0.42$; in 500 mM NaCl, $D_t^0 = 13.7\ (\pm 0.4) \times 10^{-8}$ cm^2 s^{-1}, $\beta = 0.32$ ml/mg, and $\upsilon = 0.50$; and in 500 mM NaOH, $D_t^0 = 12.8\ (\pm 0.6) \times 10^{-8}$ cm^2 s^{-1}, $\beta = 0.06$ ml/mg, and $\upsilon = 0.83$. In NaOH, the results predict the longest HA correlation lengths (Fig. 7, *inset*). At low HA concentration, the correlation lengths were predicted to be significantly shorter in deionized water than in 500 mM NaCl, but as the HA concentration increased, the calculated mesh dimensions in deionized water and 500 mM NaCl become similar.

DISCUSSION

The intrinsic stiffness of HA in solution may result from many different effects, including electrostatic interactions and the formation of intramolecular hydrogen bonds bridg-

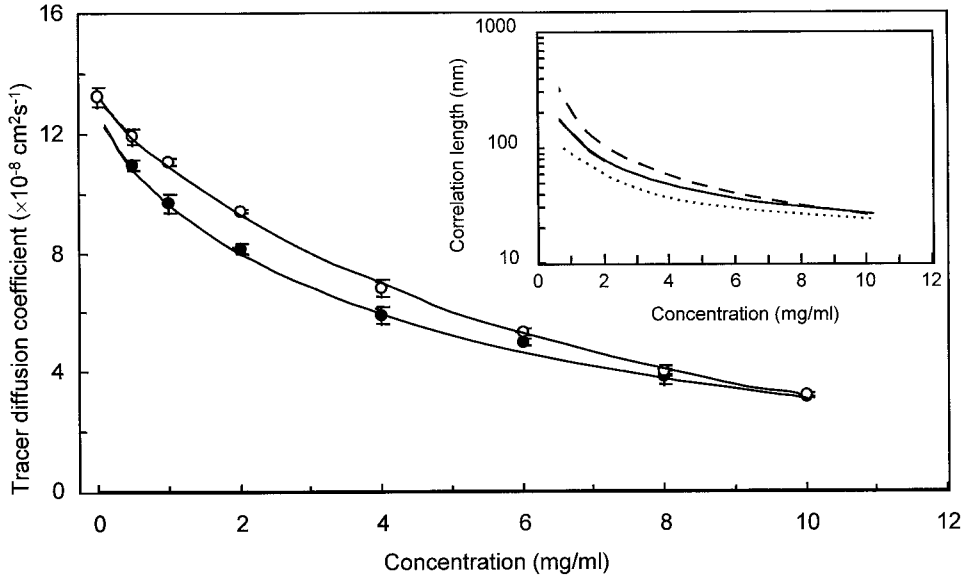

FIGURE 6 Lateral translational tracer-diffusion coefficient of 2000 kDa FITC-dextran versus concentration of 930 kDa HA (○) and 2050 kDa HA (●). Fits to Eq. 2 are shown as solid lines. The inset shows the correlation length parameter (ξ) versus HA concentration for 2050 kDa HA (*solid line*) 930 kDa HA (*long-dashed line*) and, for comparison, data taken from De Smedt et al. (1995) for 487 kDa FITC-dextran diffusing in 680 kDa HA (*short-dashed line*). All measurements in PBS at 25°C.

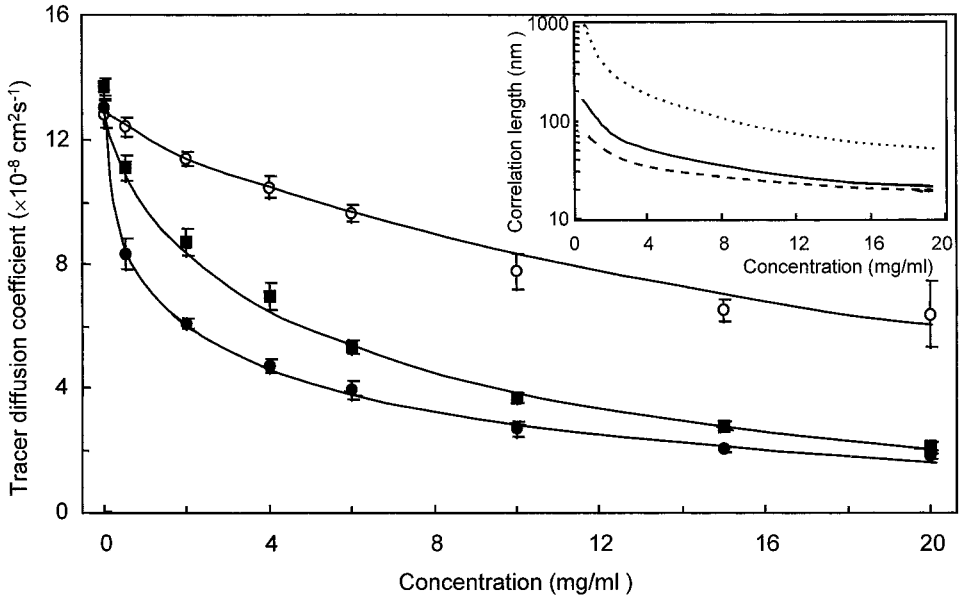

FIGURE 7 Lateral translational tracer-diffusion coefficient of 2000 kDa FITC-dextran versus concentration of 930 kDa HA for solutions in zero-added NaCl (●), 500 mM NaCl (■), and 500 mM NaOH (○). The inset shows the correlation length parameter (ξ) versus HA concentration for zero-added NaCl (*solid line*), 500 mM NaCl (*long-dashed line*), and 500 mM NaOH (*short-dashed line*). All measurements in PBS at 25°C.

ing adjacent monosaccharides (Winter and Smith, 1975; Scott and Tigwell, 1975; Atkins et al., 1980; Scott et al., 1981, 1991; Sheehan and Atkins, 1983; Cowman et al., 1984, 1996; Scott, 1992; Laurent, 1995; Almond et al., 1997, 1998a). Molecular modeling approaches have led to the proposal that hydrophobic regions on HA chains, when aligned by their secondary structure, could cause chain-chain association that would contribute to the solution properties (Scott, 1992). More recently, molecular dynamics simulations of HA oligosaccharides in water have predicted the rapid formation and loss of up to 10 separate hydrogen bonds between adjacent saccharides, with up to six present simultaneously (Almond et al., 1997, 1998b), but with none present continuously. This presents a model of a chain conformation that is stiffened by a "time average" of hydrogen bonds between adjacent saccharides.

The confocal-FRAP technique provides an experimental method for characterizing solutions at high concentration and under conditions that would favor chain-chain association. The observed reductions in the free diffusion coefficient of FA-HA, with increasing molecular weight (Fig. 1), are consistent with descriptions of partially non-free draining chain properties (Cleland, 1984; Ghosh et al., 1990; Almond et al., 1998b). The lateral translational self-diffusion coefficients of FA-HA showed a progressive fall with increasing concentration at below and above the predicted c^* (Fig. 1). Similar smooth transitions among dilute, semidilute, and concentrated regimes have been observed experimentally in many polymer/solvent systems (Callaghan and Pinder, 1984; Phillies, 1989; Imhoff et al., 1994) including HA solutions (Wik and Comper, 1982). A positive dependence of the mutual diffusion coefficient of HA (z-averaged) between 0.05 and 1.0 mg/ml has been reported using DLS (Ghosh et al., 1990). DLS analyses are sensitive to intramolecular segmental motions that do not result in translational displacements and are further complicated by disputed reports of "ordinary" and "extraordinary" phase behavior (Schmitz et al., 1984; Ghosh et al., 1992). However, confocal-FRAP measurements are independent of such effects. The hydrodynamic scaling model (Eq. 1) predicts α is proportional to molecular weight, and ν equals 0.5 for high molecular weight polymers (Phillies, 1989). This is not apparent in the present results, and although all data fit the form of Eq. 1, and α and ν fall within accepted values (Phillies, 1989), it suggests that Eq. 1 does not provide a complete description of HA behavior.

Contraction of the HA domain due to increased charge shielding results in a 2.8-fold increase in FA-HA self-diffusion with increasing NaCl concentration (Fig. 2). This change is similar to that observed in some DLS studies (Reed et al., 1989), and is consistent with reduced R_g, viscosity, and increased sedimentation coefficients (Sheehan et al., 1983: Wik and Comper, 1982). Other DLS studies on HA report no increase in the mutual diffusion coefficient (z-averaged), with increases in ionic strength (Ghosh et al., 1993). The apparent incompatibility may be because, as noted above, effects other than hydrodynamic friction influence DLS data. The contribution of electrostatic effects to macromolecular stiffness under physiological conditions of ionic strength and pH is suggested to be small, as the contraction of the HA molecular domain is largely complete in going from zero to 100 mM NaCl (Figs. 2 and 3).

The effect of NaOH is to further contract the domain size of FA-HA, supplementary to the reduction found due to electrostatic shielding (Fig. 3). This effect is reversible and is consistent with previously reported reductions in R_g and intrinsic viscosity (Ghosh et al., 1993). Changes in the R_h and hydrodynamic volume of FA-HA with NaCl and NaOH were calculated using the Stokes-Einstein approximation for

the behavior of a sphere:

$$D_0 = \frac{\kappa T}{6\pi\eta R_h} \quad (4)$$

where κ is Boltzmann's constant, T is temperature, and η is the solvent. If it is assumed that the self-diffusion coefficient at 0.2 mg/ml is approximately equal to the free diffusion coefficient (Fig. 1), then from the Stokes-Einstein equation, R_h contracted from 95 nm to 33.5 nm in going from deionized water to 500 mM NaCl (Fig. 3), reducing further to 17.5 nm in 500 mM NaOH. In going from 0.5 M NaOH into deionized water, the apparent domains of HA chains are increased by >100 times and this is most likely to result from increased electrostatic interactions and hydrogen bond formation. In the most compact configuration in alkali, the hydrodynamics of FA-HA become similar to those of the partly branched FITC-dextran (2000 kDa, R_h = 19 nm), which is neither charged nor predicted to form comparable hydrogen bonds. This major change in the hydrodynamic properties of HA in alkali has a profound impact on the intermolecular interactions in more concentrated solutions, as observed for 830 kDa FA-HA at 2 and 10 mg/ml (Fig. 4). For HA of 500 kDa in 0.5 M NaOH (Fig. 3), domain overlap is predicted to occur at 37 mg/ml. This implies that at 2–10 mg/ml solutions are well below c^*, and this is entirely consistent with the comparatively greater network mobility observed in self-diffusion experiments (Fig. 5).

Tracer diffusion results at low HA concentrations (Fig. 7) show analogous behavior to the changes in self-diffusion (Fig. 2). The network is both more permeable and more mobile in 0.5 M NaCl than in deionized water, and this supports a model involving contraction of the HA chain conformation in the presence of increasing electrolyte. However, as the concentration of HA approached 10 mg/ml (Fig. 7), tracer mobility became progressively independent of salt concentration, indicating that at high concentration chain density is the major determinant of matrix permeability. The lack of a salt effect at high HA concentration is interesting, as it may suggest a lack of hydrophobic interactions between chains (see below).

Tracer diffusion studies demonstrated that below 6 mg/ml, 2000 kDa FITC-dextran was less mobile in 2050 kDa HA than 930 kDa HA. However, tracer mobility was independent of HA molecular weight at 10 mg/ml, suggesting HA chain density determines solute mobility at this concentration regime at physiological pH (Fig. 6). Tracer studies also provide a measure of the major changes induced by NaOH. In HA (930 kDa), at 20 mg/ml (Fig. 7), the FITC-dextran translational diffusion is independent of NaCl concentration, but not of NaOH concentration. This suggests that 20 mg/ml represents a semi-dilute regime in the presence of NaOH, whereas it is clearly a concentrated, entanglement-dominated regime in NaCl and in deionized water. The solution properties at higher concentration can therefore be directly related to the hydrodynamic volumes of single chains. Results at high pH, showing the greater mobility and permeability of HA, clearly reveal the degree to which, at neutral pH, intrachain hydrogen bonds profoundly affect chain stiffness, chain entanglement, and interchain hydrodynamic interactions.

The changes in self-diffusion of HA observed at different ionic strength or at alkaline pH are accompanied by similar changes in the permeability of the HA network to the high molecular weight FITC-dextran probe. Tracer- and self-diffusion do not necessarily arise from similar mechanisms, although both can be described phenomenologically by the stretched exponential-type scaling equation. To provide a physical basis for Eqs. 1 and 2, Phillies (1989) modeled polymer-polymer interactions assuming interactions are self-similar, and dominated by hydrodynamic forces rather than entanglement or topological effects. The model predicts for self-diffusion, $\alpha \propto (M_{polymer})^1$, and for tracer diffusion, $\beta \propto (M_{polymer} \times M_{probe})^{0.5}$. When polymer-polymer hydrodynamic coupling resembles polymer-probe coupling, then α should approximately equal β. In 500 mM NaCl α = 0.26 and β = 0.32, and in 500 mM NaOH α = 0.07 and β = 0.06. The agreement between α and β suggests that dextran-HA hydrodynamic interactions resemble HA-HA at high salt concentrations and at high pH, which is consistent with the counterion-induced polyelectrolyte destiffening. The lower values of α and β in alkali are consistent with there being much less intermolecular hydrodynamic interaction, and this is consistent with a contracted and flexible HA macromolecular conformation in which both electrostatic interactions and intramolecular hydrogen bonding are minimized. In deionized water, tracer and self-diffusion are dissimilar with α = 0.18 and β = 0.58, and under these conditions the results are consistent with HA being in a highly extended and stiffened form.

The present results, made under conditions of high concentration and at equilibrium in solutions at zero shear, should favor the detection of stable, or multiple, weak chain-chain interactions. However, if there were chain-chain associations mediated by hydrophobic interactions, they would be favored by increasing electrolyte (cf. DNA and RNA), particularly at high concentration, and this would give lower translational diffusion coefficients in 0.5 M NaCl compared with deionized water (Fig. 5), and it would also create a less permeable barrier to tracer diffusion (Fig. 6). The absence of any such effects in the present results thus suggests that self-association of HA through mechanisms such as hydrophobic patches (Scott, 1992), does not contribute significantly to HA solution properties. This is further supported by the absence of transitions in the temperature dependence of lateral translational diffusion of FA-HA. Recent viscometric studies with short HA chains (Fujii et al., 1996), and calorimetric studies of heats of dilution of HA and hydrophobic derivatives of HA (Geciavo et al., 1995), have also shown no evidence for concentration-dependent, hydrophobically stabilized, inter or intrachain associations.

The data presented in this study suggest that hydrogen bonds and polyanionic properties of HA both contribute to provide a highly expanded macromolecular conformation. However, under physiological conditions of ionic strength the results predict the electrostatic effects to be modest and the major contribution to the large hydrodynamic volume of HA

and hence its other important non-Newtonian viscoelastic properties are due to hydrogen bonding between adjacent saccharides. This restricts rotation and flexion at the glycosidic bonds and creates a stiffened polymer chain. The flexibility and permeability properties of the HA network can then be accounted for in terms of interchain hydrodynamic interactions of this extended structure, with entanglement being especially important at elevated concentrations. However, even at high concentrations, under physiological conditions, individual HA chains remain mobile and at no stage do HA solutions undergo transition to a gel-like state. These observations appear incompatible with any significant degree of intermolecular association that is stable or cooperative. The results suggest that even at high concentrations a simple hydrodynamic model with chains stiffened by hydrogen bonds accounts for the major solution properties of HA.

We thank The Wellcome Trust and Seikagaku Corp. (Tokyo) for support.

REFERENCES

Almond, A., A. Brass, and J. K. Sheehan. 1998a. Deducing polymeric structure from aqueous molecular dynamics simulations of oligosaccharides: predictions from simulations of hyaluronan tetrasaccharides compared with hydrodynamic and x-ray fibre diffraction data. *J. Mol. Biol.* 284:1425–1437.

Almond, A., A. Brass, and J. K. Sheehan. 1998b. Dynamic exchange between stabilized conformations predicted for hyaluronan tetrasaccharides: comparison of molecular dynamics simulations with available NMR data. *Glycobiology*. 8:973–980.

Almond, A., J. K. Sheehan, and A. Brass. 1997. Molecular dynamics simulations of the disaccharides of hyaluronan in solution. *Glycobiology*. 7:597–604.

Atkins, E. D. T., D. Meader, and J. E. Scott. 1980. Model of hyaluronic acid incorporating four intramolecular hydrogen bonds. *Int. J. Biol. Macromol.* 2:318–319.

Callaghan, P. T., and D. N. Pinder. 1984. Influence of multiple length scales on the behaviour of polymer self-diffusion in the semidilute region. *Macromolecules.* 17:431–437.

Cleland, R. L. 1968. Ionic polysaccharides. II. Comparison of polyelectrolyte behaviour of hyaluronate with that of carboxymethyl cellulose. *Biopolymers.* 6:1519–1529.

Cleland, R. L. 1984. Viscometry and sedimentation equilibrium of partially hydrolyzed hyaluronate: comparison with theoretical models of worm-like chains. *Biopolymers*. 23:1379–1385.

Coleman, P. J., D. Scott, A. Abiona, D. E. Ashhurst, R. M. Mason, and R. J. Levick. 1998. Action of specific hyaluronidases on hydraulic conductance of interstitium in rabbit knee synovium. *J. Physiol.* 509:695–710.

Comper, W. D., and O. Zamparo. 1990. Hydrodynamic properties of connective tissue polysaccharides. *Biochem. J.* 269:561–564.

Cowman, M. K., D. Cozart, K. Nakanishi, and E. A. Balazs. 1984. ^{1}H-NMR of glycosaminoglycans and hyaluronic acid oligosaccharides in aqueous solutions: the amide proton environment. *Arch. Biochem. Biophys.* 230:203–212.

Cowman, M. K., D. M. Hittner, and J. Feder-Davies. 1996. ^{1}C-NMR studies of hyaluronan: conformational sensitivity to various environments. *Macromolecules.* 29:2894–2902.

De Gennes, P. G. 1974. Scaling Concepts in Polymer Physics. Cornell University Press, Ithaca, NY.

De Smedt, S. C., A. Lauwers, J. Demeester, Y. Engelborghs, G. De May, and M. Du. 1994. Structural information on hyaluronic acid solutions as studied by probe diffusion experiments. *Macromolecules.* 27:141–146.

Fosang, A. J., and T. E. Hardingham. 1996. Matrix proteoglycans. *In* Extracellular Matrix, Vol. 2. W. D. Comper, editor. Harwood Academic Publishers, Amsterdam, The Netherlands. 200–229.

Fujii, K., M. Kawate, Y. Kobayashi, A. Okamoto, and A. Okamoto. 1996. Effects of the addition of hyaluronate segments with different chain lengths on the viscoelasticity of hyaluronic acid solutions. *Biopolymers*. 38:583–591.

Geciavo, R., A. Flaibani, F. Delben, G. Liut, R. Urbani, and A. Cesaro. 1995. Physico-chemical properties of hyaluronan and its hydrophobic derivatives: a calorimetric study. *Macromol. Chem. Phys.* 196:2891–2903.

Ghosh, S., I. Khobal, D. Zanette, and W. F. Reed. 1993. Conformational contraction and hydrolysis of hyaluronate in sodium hydroxide solutions. *Macromolecules.* 26:4684–4691.

Ghosh, S., R. M. Peitzsch, and W. F. Reed. 1992. Aggregates and other particles as the origin of the extraordinary diffusional phase in polyelectrolyte solutions. *Biopolymers*. 8:1105–1122.

Ghosh, S., L. Xiao, C. E. Reed, and W. F. Reed. 1990. Apparent persistence lengths and diffusion behaviour of high molecular weight hyaluronate. *Biopolymers*. 30:1102–1112.

Glabe, C. G., P. K. Harty, and S. D. Rosen. 1983. Preparation and properties of fluorescent polysaccharides. *Anal. Biochem.* 130:287–294.

Gribbon, P., and T. E. Hardingham. 1998. Macromolecular diffusion of biological polymers measured by confocal fluorescence recovery after photobleaching. *Biophys. J.* 75:1032–1039.

Imhoff, A., A. Van Blaadren, G. Maret, J. Mallema, and J. K. G. Dhont. 1994. A comparison between the long time self diffusion of and low shear viscosity of concentrated dispersions of charged colloidal silica spheres. *J. Chem. Phys.* 100:2170–2181.

Kubitscheck, H., P. Wedekind, and R. Peters. 1994. Lateral diffusion measurements at high spatial resolution by scanning microphotolysis in a confocal microscope. *Biophys. J.* 67:946–965.

Laurent, T. C. 1995. Structure of the extracellular matrix and the biology of hyaluronan. *In* Interstitium, Connective Tissue and Lymphatics. R. K. Reed, N. G. McHale, J. L. Bert, C. P. Winlove, and G. A. Laine, editors, Portland Press, London, 1–12.

Morris, E. R., D. A. Rees, and E. J. Welsh. 1980. Conformation and dynamic interactions in hyaluronan solutions. *J. Mol. Biol.* 138:383–400.

Phillies, D. J. 1989. The hydrodynamic scaling model for polymer self-diffusion. *J. Phys. Chem.* 93:5029–5039.

Reed, W. F. 1996. Data evaluation for unified multi-detector size-exclusion chromatography, molar mass, and radius of gyration. *Macromol. Chem. Phys.* 197:1539–1575.

Reed, C. E., X. Li, and W. F. Reed. 1989. The effects of pH on hyaluronate as observed by light scattering. *Biopolymers*. 28:1981–2000.

Schmitz, K. S., M. Lu, N. Singh, and D. J. Ramsey. 1984. Ordinary extraordinary phase transition of poly(lysine)–comments. *Biopolymers*. 23:1637–1646.

Scott, J. E. 1992. Supramolecular organisation of extracellular matrix, glycosaminoglycans, in vitro and in the tissues. *FASEB J.* 6:2639–2645.

Scott, J. E., C. Cummings, A. Brass, and Y. Chen. 1991. Secondary and tertiary structures of hyaluronan in aqueous solution, investigation by rotary shadowing electron microscopy and computer simulation. *Biochem. J.* 274:699–705.

Scott, J. E., F. Heatley, D. Moorcroft, and A. H. Olaveson. 1981. Secondary structures of hyaluronate and chondroitin sulphates. *Biochem. J.* 199:829–832.

Scott, J. E., and M. J. Tigwell. 1975. The influence of the intrapolymer environment on periodate oxidation of uronic acids in polyuronides and glycosaminoglycuronans. *Biochem. Soc. Trans.* 3:662–664.

Sheehan, J. K., C. Arundel, and C. F. Phelps. 1983. Effect of the cations sodium, potassium and calcium on the interactions of hyaluronate chains: a light scattering and viscometric study. *Int. J. Biol. Macromol.* 5:222–228.

Sheehan, J. K., and E. D. T. Atkins. 1983. X-ray fiber diffraction study of the conformational changes in hyaluronic acid induced in the presence of sodium, potassium and calcium cations. *Int. J. Biol. Macromol*. 5:215–221.

Wik, K. O., and W. D. Comper. 1982. Hyaluronate diffusion in semi-dilute solutions. *Biopolymers*. 21:583–599.

Winter, W. T., and P. J. C. Smith. 1975. Hyaluronic acid: structure of a fully extended 3-fold helical sodium salt and comparison with the less extended 4-fold helical forms. *J. Mol. Biol.* 99:219–235.